Cell Biochem Biophys (2013) 67:1103–1113
DOI 10.1007/s12013-013-9614-8

ORIGINAL PAPER

PT-ACRAMTU, A Platinum–Acridine Anticancer Agent, Lengthens and Aggregates, but does not Stiffen or Soften DNA

Samrat Dutta · Matthew J. Snyder · David Rosile · Kristen L. Binz · Eric H. Roll · Jimmy Suryadi · Ulrich Bierbach · Martin Guthold

Published online: 1 May 2013

Abstract We used atomic force microscopy (AFM) to study the dose-dependent change in conformational and mechanical properties of DNA treated with PT-ACRAMTU ([PtCl(en)(ACRAMTU-S)]$(NO_3)_2$, (en = ethane-1,2-diamine, ACRAMTU = 1-[2-(acridin-9-ylamino)ethyl]-1,3-dimethylthiourea. PT-ACRAMTU is the parent drug of a family of non-classical platinum-based agents that show potent activity in non-small cell lung cancer in vitro and in vivo. Its acridine moiety intercalates between DNA bases, while the platinum group forms mono-adducts with DNA bases. AFM images show that PT-ACRAMTU causes some DNA looping and aggregation at drug-to-base pair ratio (r_b) of 0.1 and higher. Very significant lengthening of the DNA was observed with increasing doses of PT-ACRAMTU, and reached saturation at an r_b of 0.15. At r_b of 0.1, lengthening was 0.6 nm per drug molecule, which is more than one fully stretched base pair stack can accommodate, indicating that ACRAMTU also disturbs the stacking of neighboring base pair stacks. Analysis of the AFM images based on the worm-like chain (WLC) model showed that PT-ACRAMTU did not change the flexibility of (non-aggregated) DNA, despite the extreme lengthening. The persistence length of untreated DNA and DNA treated with PT-ACRAMTU was in the range of 49–65 nm. Potential consequences of the perturbations caused by this agent for the recognition and processing of the DNA adducts it forms are discussed.

Keywords Acramtu · Cancer drug · DNA lengthening · Persistence length

Introduction

DNA is the major target of numerous anticancer drugs, and many of these DNA-targeting agents induce conformational changes in the DNA such as bending and unwinding of the double helix. These conformational changes can have different effects on cells. They can trigger apoptosis [1], the desired outcome in cancer treatment. However, the drug-induced DNA damage may also get repaired by the cellular DNA repair machinery, which can result in cancer cell survival and tumor resistance to the applied drug [2, 3]. Anticancer drugs may also cause permanent mutations with uncertain outcomes. In many cases, the drug-induced damage is detected by proteins of the DNA repair machinery, which recognize bulky adducts and the distortions caused by them [2].

Cisplatin, a DNA-targeting agent, has been widely investigated and used as a chemotherapeutic against testicular and ovarian cancer during the last 30 years [4]. Cisplatin binds preferentially to neighboring purine bases of the same DNA strand in the DNA major groove, thus producing bifunctional adducts (mainly GG and 5′-AG cross-links), which causes the DNA to bend toward the major groove [5, 6]. In spite of its impressive success rates in testicular and ovarian cancers, cisplatin has shown limited success in the treatment of other types of cancer, such as non-small cell lung cancer [7]. One of the major drawbacks of existing cancer chemotherapeutics, such as

Samrat Dutta and Matthew J. Snyder contributed equally to this study.

S. Dutta · M. J. Snyder · D. Rosile · K. L. Binz · E. H. Roll · M. Guthold (✉)
Department of Physics, Wake Forest University, Winston-Salem, NC 27109, USA
e-mail: gutholdm@wfu.edu

J. Suryadi · U. Bierbach
Department of Chemistry, Wake Forest University, Winston-Salem, NC 27109, USA

cisplatin, is that the cytotoxic lesions they produce in genomic DNA are recognized and repaired by the cellular machinery [3], thereby conferring resistance to the specific drug. Thus, one aim in developing new cancer therapeutics is to induce structural changes in the DNA that are not recognized or repairable by the DNA repair machinery, but which are able to induce apoptosis.

PT-ACRAMTU ($[PtCl(en)(ACRAMTU)](NO_3)_2$, (en = ethane-1,2-diamine, ACRAMTU = 1-[2-(acridin-9-ylamino)ethyl]-1,3-dimethylthiourea; Fig. 1) is the prototype of a family of inorganic–organic hybrid agents that have shown promising cytotoxicity in various solid tumor cell lines and a mouse model, in particular non-small-cell lung cancer [8–10]. PT-ACRAMTU-type compounds are thought to stall DNA processing enzymes by unwinding and lengthening the DNA molecule [11]. PT-ACRAMTU binds to the DNA through intercalation of the acridine ring between the DNA base pair and monofunctional platination of the purine bases with a preference for 5′-TA, 5′-CG and 5′-GA sites [12]. Although significant progress has been made toward understanding the interaction of PT-ACRAMTU with DNA [12–15], the changes in the mechanical and conformational properties of DNA due to its interaction with PT-ACRAMTU are not yet fully understood. Gel mobility shift assays showed that PT-ACRAMTU-treated DNA molecules migrate slower as compared to untreated DNA [11], but it is unclear if the differences in mobility are caused by an increase in DNA length, rigidity (persistence length), DNA bending, the additional positive charges, or a combination of these factors. It has been shown that these DNA mechanical and conformational properties can have a significant effect on DNA repair [16], transcription [17], and replication [18, 19]. Therefore, investigating the mechanical and conformational changes caused by PT-ACRAMTU may provide insights into the mode of action of this promising drug.

Atomic force microscopy (AFM) imaging is a technique that can be used to quantify protein- or drug-induced changes in DNA conformation [20, 21]. Rivetti et al. [22, 23] showed that under certain deposition conditions, DNA molecules equilibrate on the substrate, that is, they maintain their lowest energy state from solution. AFM is particularly well suited to determine protein- or ligand-induced bend angles, changes in contour length, changes in the end-to-end distance, or changes in persistence length [22, 24]. Persistence length is a measure of DNA stiffness, and is a quantity used to describe the conformation of DNA molecules in the worm-like chain (WLC) model. In this model, DNA is treated as a semi-flexible rod that gently bends (curves) due to thermal fluctuation. The resulting deviation from a straight line, θ, between two segments separated by a distance, l, is given by $< \cos \theta >_{2D} = e^{-l/2P}$, where P is the persistence length (this is the equation for molecules that have equilibrated in two dimensions; the equation for molecules in three dimensions is $< \cos \theta >_{3D} = e^{-l/P}$). For large values of P, DNA behaves like a stiff rod and the thermally induced bending is small. Conversely, more flexible DNA is characterized by shorter persistence lengths.

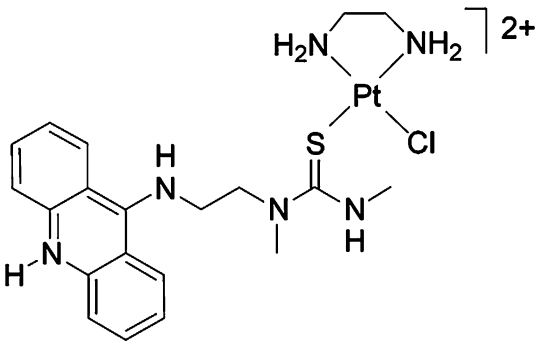

Fig. 1 Chemical structure of PT-ACRAMTU. The acridine moiety intercalates between base pairs, whereas the metal forms a covalent mono-adduct with an adjacent nucleobase. The molecule has an overall 2+ charge

Using AFM imaging, we investigated the dose-dependent effects of PT-ACRAMTU on the conformation and mechanical properties of a DNA fragment. Specifically, we determined its contour length, L, the persistence length, P, and aggregation propensity for various degrees of modification with PT-ACRAMTU (expressed as ratio of drug per base pairs, r_b). In our experiments, r_b ranged from 0 to 0.3. We found that at $r_b = 0.1$ PT-ACRAMTU lengthens the DNA by 0.6 nm per intercalated drug molecule—an amount larger than a maximally stretched single stack of base pairs. At higher concentrations ($r_b > 0.1$), PT-ACRAMTU causes some intramolecular looping and aggregation of the DNA molecules. For $r_b > 0.15$, saturation of available binding sites with PT-ACRAMTU is observed. At the highest concentrations, $r_b = 0.3$, PT-ACRAMTU seems to weaken DNA, as the DNA molecules sometimes, but not always, appear to have gaps in the AFM images. The gaps are probably induced by the physical interaction of the AFM probe with the weakened DNA, as the probe scans (and taps on) the DNA. We also determined that PT-ACRAMTU does not significantly change the persistence length at any of the concentrations (for non-aggregated DNA).

Materials and Methods

Platination Reactions

A 1,154-bp linear DNA fragment was amplified from a circular DNA pDSP (6,136 bp) by polymerase chain reaction. A region between position 1901 (plus an appended AGCTT Hind III site) and position 3049 was amplified with primer 1 (1154 forward: 5′-AGC TT-A GGT GAG

AAC ATC CCT GC and primer 2 (1154 reverse: 5′-AGC TTG CAT GCC TGC AGG). The sequence was confirmed by sequencing (Genewiz, South Plainfield, NJ). The fragment was gel-purified, and stored in TE buffer (10 mM Tris–HCl,1 mM EDTA, pH 7.4; all chemicals from Sigma-Aldrich, USA, unless otherwise noted). Concentrations of DNA and PT-ACRAMTU (ε_{413} = 9,450 M^{-1} cm^{-1}) [25] were calculated from UV/visible absorption spectra (Cary 50 Bio, Varian, USA). Reactions of the DNA fragment with PT-ACRAMTU were performed in deionized water at 37 °C in the dark for 24 h. The long incubation assures that the reaction goes to completion; the half-life of the nucleobase platination is 83 min [26]. Subsequently, samples were dialyzed against deionized water at 4 °C for 6–12 h in the dark (cellulose ester membrane, 3,500 Da MWCO, Pierce Biotechnology, Rockford, IL)].

AFM imaging and analysis

1–5 μL of the untreated DNA or PT-ACRAMTU-treated DNA stock solution, were diluted with 10 μL DNA deposition buffer (4 mM HEPES, 2 mM $MgCl_2$, 10 mM NaCl, pH 7.4) to a final concentration of 2 nM. 10 μL of this solution were deposited on a 1 cm^2, freshly cleaved muscovite mica surface (Paramount Corporation, New York, NY). After 2 min the mica surface was thoroughly rinsed with deionized water followed by drying in a gentle flow of dry nitrogen. Imaging was done with a Nanoscope IIIa (Veeco Instruments, USA) using stiff AFM probes (Nanosensors, spring constant, k = 21–98 N/m; resonance frequency, f = 146–236 kHz) in tapping mode at a scanning frequency of 1–3 Hz. DNA molecules were imaged by scanning over an area of 1.5 μm^2. Images were acquired by scanning with 512 × 512 pixels. Therefore, the size of each image pixel is 2.93 nm^2. 583 untreated DNA molecules, and 521, 587, 337, 109, and 133 PT-ACRAMTU-treated DNA molecules, for r_b values 0.02, 0.05, 0.1, 0.2, and 0.3, respectively, were analyzed. The analysis of the AFM images was conducted using MATLAB (version 7.12.0, The MathWork, Inc, USA) software ALEX. Image processing and analysis of single DNA molecules using ALEX has been reported in [22, 24]. In brief, the software transforms the image integer values of the Nanoscope files into nanometer using the calibration relations in the Nanoscope III documentation. Prior to analysis, the image files were flattened to remove tilt or slope of the substrate. To measure L, the pixels of the DNA molecule were traced; then the coordinates of each pixel of a DNA molecule were smoothed by fitting the traces to a 5th degree polynomial and saved as coordinate files. To study the flexibility (persistence length, P) of DNA molecules for various doses of PT-ACRAMTU, we used the following method. For two-dimensionally equilibrated molecules, the angle between two segments separated by a distance, l, is given by [22]:

$$<\theta^2>_{2D} = 1/P. \quad (1)$$

Thus, when plotting $<\theta^2>$ versus l, the slope is the inverse of the persistence length. The segment length, l, in these plots runs from a few nanometers in length to several hundred nanometers. Thus, tens or hundreds of DNA fragments can give thousands of data points, and good statistics can be achieved. This type of analysis, as described by Rivetti et al. [22], is well accepted for analyzing DNA persistence length and has been vetted by numerous researchers. A related method to determine the persistence length of DNA molecules involves the end-to-end distance, R, of the DNA molecules on the surface [22]. The mean squared end-to-end distance $<R^2>$, averaged over many molecules, is given by $\langle R^2 \rangle_{2D} = 4PL\left(1 - \frac{2P}{L}\left(1 - e^{-\frac{L}{2P}}\right)\right)$, where L is the contour length of the molecule. Measuring R and L from the AFM images, thus, allows determination of P. However, this method has typically a larger uncertainty, requiring measurements on hundreds of molecules. Using Eq. (1) is, thus, preferred.

Results

Samples of untreated DNA and DNA containing PT-ACRAMTU adducts at various degrees of modification were diluted in deposition buffer and deposited onto a mica surface. Under our deposition conditions, DNA equilibrates on a two dimensional mica surface and maintains its worm-like chain behavior [22]. Since deposited DNA behaves like an equilibrated molecule in a 2-D solution, it is possible to determine parameters that define the DNA conformation, such as the persistence length, P, bend angle, β, contour length, L, or the end-to-end distance R [22, 27]. Using AFM, we imaged untreated and PT-ACRAMTU-treated DNA molecules. The analysis of these molecules was based on polymer chain statistics and the WLC model, which describes DNA as a semi-flexible polymer [27–32]. Figure 2 shows AFM images of untreated DNA molecules and the molecules treated with PT-ACRAMTU. The image of untreated DNA molecules (Fig. 2a) shows uniformly dispersed molecules. Figure 2b–f shows representative images of DNA molecules treated with different doses of PT-ACRAMTU ranging from r_b = 0.02 to r_b = 0.3. A first visual inspection shows that PT-ACRAMTU treated DNA molecules maintain a similar curvilinear shape as observed for untreated DNA. However, closer analysis reveals several significant dose-dependent differences.

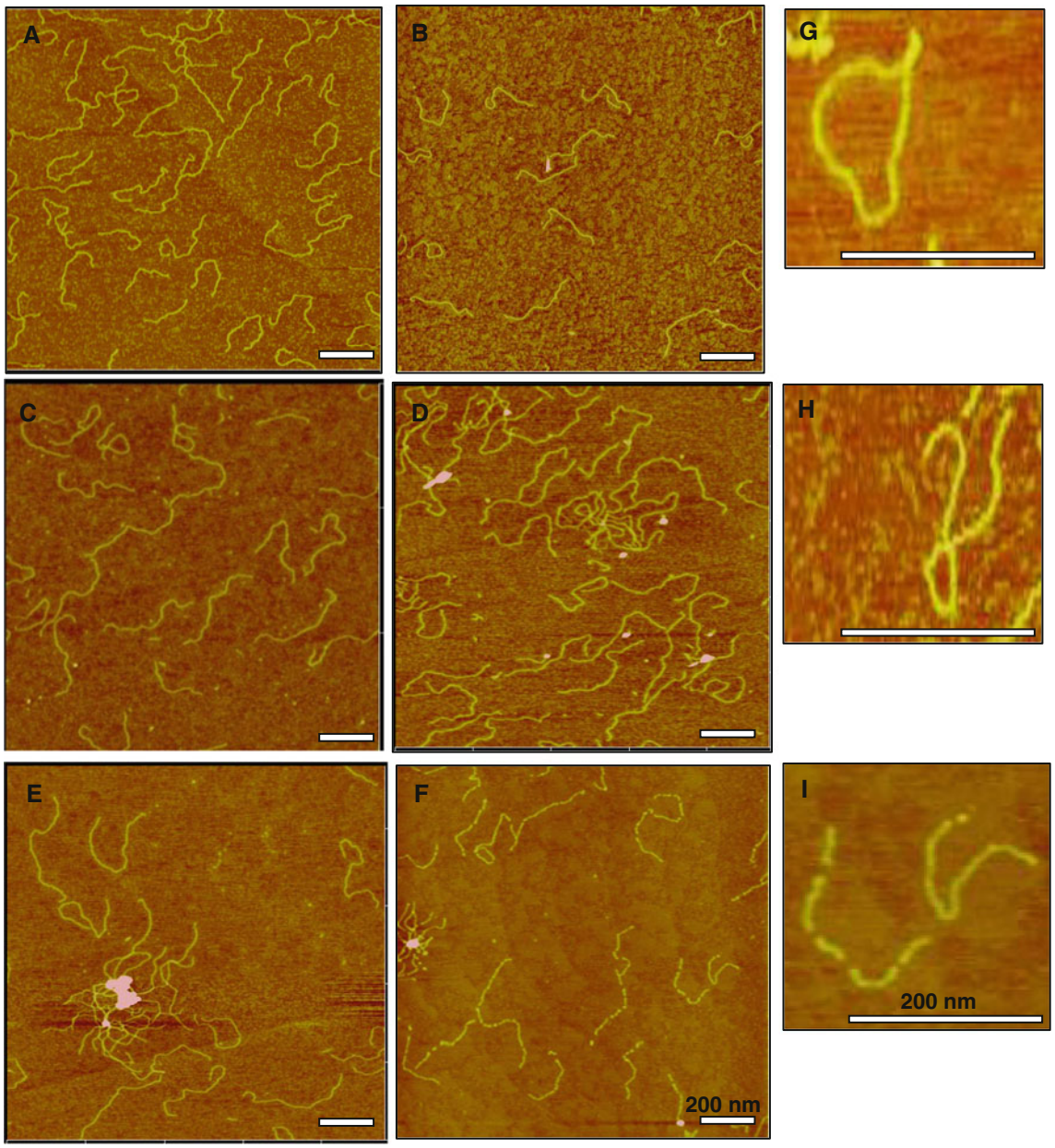

Fig. 2 AFM images of 1,154 bp DNA fragment. **a** Untreated DNA; DNA treated with different doses of PT-ACRAMTU **b** 0.02 r_b, c 0.05 r_b, **d** 0.1 r_b, **e** 0.2 r_b, **f** 0.3 r_b, **g–i** *Zoomed images* show DNA looping and double-strand breaks. The *scale bar* in all images is 200 nm

Increasing Aggregation

Especially at higher PT-ACRAMTU concentrations, we observed some loop formation and significant aggregation of DNA molecules. This effect is most likely caused by the 2+ charge on the PT-ACRAMTU molecule, and has also been reported with other positively charged DNA intercalators [33]. The platinum-treated DNA molecules showed minimal amounts of intramolecular looping and aggregation for smaller doses (r_b, 0.02–0.05), indistinguishable from untreated DNA molecules. The molecules treated with higher doses (r_b, 0.1, 0.2, 0.3) showed significant aggregation (Fig. 2e, f). A quantitative analysis revealed that the percentage of aggregated molecules increases from background level (r_b, 0.02–0.05) to 11, 21, and 24 %, for r_b values of 0.1, 0.2, and 0.3, respectively (Fig. 3). To determine the percentage of aggregated molecules, we counted the number of free molecules and calculated the number of molecules in aggregates from the total DNA contour length in an aggregate divided by the contour length of a single molecule. After the interaction of PT-ACRAMTU with DNA has reached a saturation phase, the cationic charge on the DNA-bound

PT-ACRAMTU would significantly reduce or completely neutralize the negative charge on the DNA phosphodiester backbone; this could cause the aggregation of DNA molecules at higher doses of the platinum drug (see discussion).

DNA Double-Strand Breaks

In addition to DNA looping and aggregation, we also observed some DNA double-strand breaks for the highest dose of PT-ACRAMTU ($r_b = 0.3$, Fig. 2f, i) We observed this repeatedly, but not always. We did not see these breaks at the lower platinum concentrations. This is an unexpected observation, since the adducts formed by divalent platinum complexes do not cleave DNA, and DNA strand breaks have not been observed in gel electrophoresis-based assays [11]. It appears that PT-ACRAMTU at very high doses may weaken the DNA, and the physical interaction with the scanning tip during AFM imaging might break the weakened DNA. Though the exact mechanism of the DNA weakening is not known, we speculate that at saturating conditions the intercalating PT-ACRAMTU strains the covalent bonds in the DNA backbone to the point at which they can break by the force applied by the AFM tip. Similar double-strand breaks have been studied before with other intercalators using bulk techniques and AFM imaging [34–36]. Thus, the source of the DNA damage observed in our experiments appears to be the result of the physical interaction (tapping) of the AFM probe with the DNA, combined with weakening by mechanical strain due to intercalation, rather than chemical DNA cleavage.

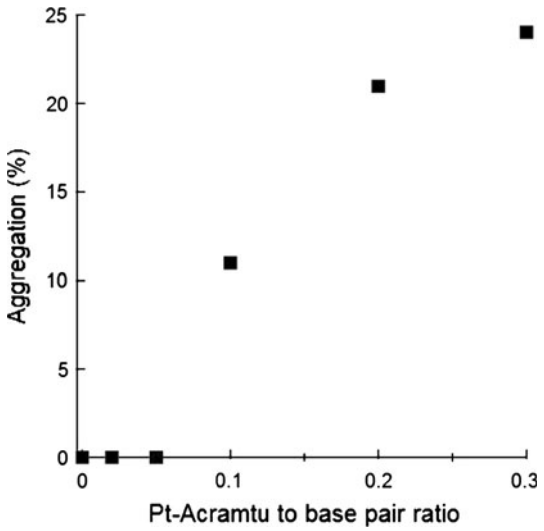

Fig. 3 Plot of DNA aggregation as a function of increasing doses of PT-ACRAMTU ($r_b = 0$–0.3). Aggregation was determined from the total length of free DNA and the total length of DNA of aggregated DNA. There was negligible aggregation for $r_b < 0.1$. Aggregation increased with increasing PT-ACRAMTU for r_b values of 0.1 and above

Lengthening of DNA, Drug Binding Saturation, and DNA Stiffness

To quantify the conformational and mechanical properties of untreated and PT-ACRAMTU-treated DNA, we determined the contour length, L, and also determined the persistence length, P, a measure of DNA stiffness, as a function of drug concentration. Figure 4 shows the contour length distributions of untreated and treated DNA. Intercalation of the acridine moiety in PT-ACRAMTU into the DNA base stack results in a distinct increase in L. Figure 4 shows a clear upward shift in the contour length L with increasing r_b. The average values for the distribution of contour lengths for the untreated DNA and for treated DNA are listed in Table 1. As mentioned above, DNA aggregation increased with higher doses of PT-ACRAMTU (Fig. 2e, f). We analyzed all molecules for which we could clearly discern the contours. Thus, DNA molecules that were looped or aggregated were excluded from this analysis. When plotting the average lengthening (average change in contour length) versus drug concentration (Fig. 5), several observations can be made. The curve has an asymmetric sigmoidal shape, indicating cooperative binding of PT-ACRAMTU to DNA. The curve could be fit very well ($R = 0.9992$) to a general sigmoidal curve, $\Delta L(r_b) = A + \frac{\Delta L_{max} - A}{1 + e^{-B(r_b - C)}}$. The best fit was obtained for $A = -4.50$, $\Delta L_{max} = 94.7$, $B = 41.6$, and $C = 0.07$. It is also apparent that PT-ACRAMTU reaches saturation at an r_b of ~ 0.15 (1 adduct per 6.7 base pairs). Investigating the region of the curve before saturation occurs the lengthening of the DNA molecules is up to 0.6 nm per added drug molecule. For example, considering the $r_b = 0.1$ data point, the DNA lengthens by 71 nm for 115 drug molecules added. The $r_b = 0.1$ data point should give the most accurate lengthening value, because saturation has not yet occurred (small amount of free drug molecules), and because it has the largest lengthening and thus the smallest relative error due to limited microscope resolution. This lengthening indicates efficient intercalation of PT-ACRAMTU.

To determine the change in the flexibility of DNA molecule after its interaction with PT-ACRAMTU, we used Eq. (1) to calculate the persistence length, P, by plotting $< \theta^2 >$ vs. l. A persistence length of 56 nm was determined for untreated DNA, which confirms that the imaged molecules represent 2-D equilibrated DNA molecules and that the integrity of the DNA remains intact on the mica surface [37]. Figure 6 shows a plot of $< \theta^2 >$ versus l for DNA molecules treated with different doses of PT-ACRAMTU. As can be seen from the plotted traces, no clear trend or significant change in the persistence length is observed at the various degrees of

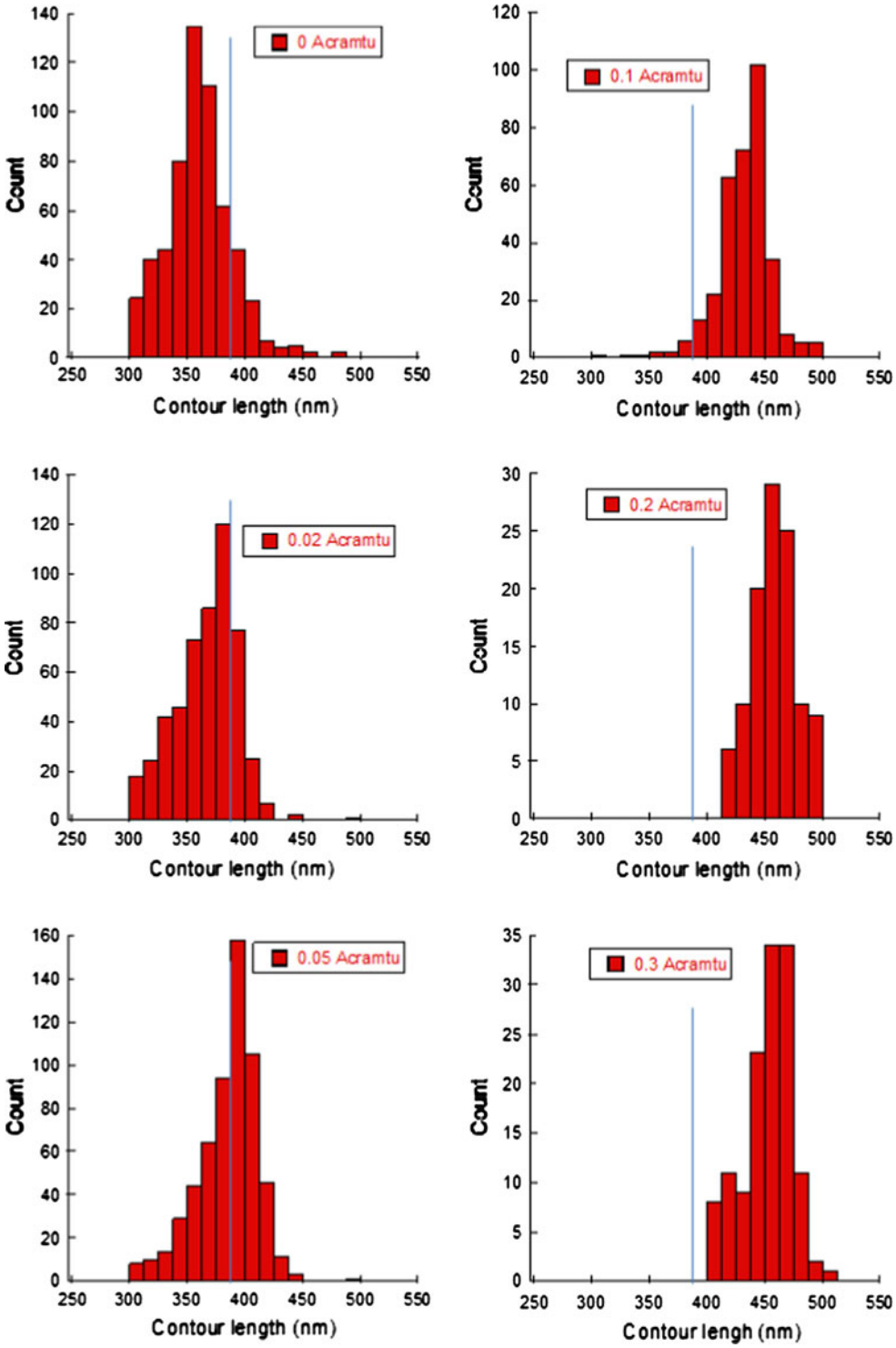

Fig. 4 Contour length distribution of untreated DNA, and DNA treated with different doses of PT-ACRAMTU ($r_b = 0$–0.3). The *blue line* represents the theoretical length of B-form DNA, 390 nm (Color figure online)

modification with platinum drug. This indicates that PT-ACRAMTU does not introduce a major change in the DNA flexibility when compared to untreated DNA, in contrast with the increase in persistence length observed for other DNA intercalators (see discussion). A summary of the L and P values is listed in Table 1.

Discussion

The prototypical anticancer drug PT-ACRAMTU and its second-generation derivatives belong to a novel class of inorganic–organic hybrid agents that kill cancer cells via a mechanism triggered by irreparable DNA damage [38].

Table 1 Summary, effect of PT-ACRAMTU on DNA conformation. PT-ACRAMTU significantly lengthens DNA, but does not have a strong (or no effect) on the stiffness of DNA (persistence length)

PT-ACRAMTU:DNA base pair ratio (r_b)	Number of molecules	Average contour length (nm)	Persistence length (nm)	Aggregation
Untreated	583	361 ± 28	56 ± 0.57	0
0.02	521	367 ± 27	52 ± 3.86	0
0.05	587	385 ± 26	65 ± 3.96	0
0.1	337	432 ± 24	49 ± 4.59	11 %
0.2	109	458 ± 19	55 ± 5.19	21 %
0.3	133	453 ± 21	56 ± 5.17	24 %

Assuming B-form DNA, and a rise of 0.338 nm/base pair, the 1,154 bp DNA would have a theoretical length of 390 nm. The persistence length of B-form DNA (random sequence) is 53 nm [22]. Values ± their standard deviations are listed. DNA molecules tend to increasingly aggregate at concentrations above r_b 0.1. For the aggregation study, we analyzed an additional 960, 311, 251 DNA molecules for r_b of 0.1, 0.2, 0.3, respectively

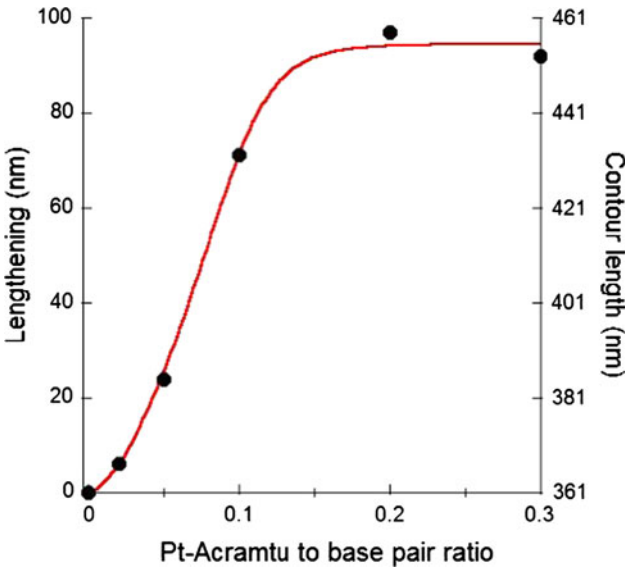

Fig. 5 Plot of the increase in DNA contour length as a function of increasing doses of PT-ACRAMTU ($r_b = 0$–0.3). The length increases sigmoidally, showing saturation at $r_b \sim 0.15$

Unlike the platinum drugs currently in clinical use, such as cisplatin, the platinum–acridines do not induce cross-links between neighboring purine bases but instead form a single covalent bond with guanine or adenine. In these monofunctional adducts, acridine intercalates between the stacked bases directly adjacent to the platinated nucleobase. This binding mode unwinds the duplex significantly but produces minimal bending and does not destabilize the duplex thermodynamically due to complete enthalpy/entropy compensation [14]. By contrast, the 1,2 intrastrand cross-link formed by cisplatin-type drugs produces a sharp kink in the damaged DNA, which is recognized by nucleotide excision repair proteins. These critical differences at the DNA level may define a novel mechanism by which the adducts formed by platinum–acridine agents circumvent tumor resistance and efficiently trigger cell death.

Previous studies on the molecular mechanism of PT-ACRAMTU have used a combination of biochemical and biophysical methods as well as high-resolution structural techniques. These studies showed DNA unwinding and an increase in the DNA length [11, 13].

The effects of some intercalators, covalent binders, and divalent ions on DNA conformation have been studied before. AFM was used to determine the lengthening by and binding constants of ethidium bromide and daunomycin [39] and Ruthenium(II) compounds [40]. Other authors have used AFM to just determine the lengthening effect of intercalators, such as echinomycin [41] and thiazole orange dimer (TOTO) [42]. Though, the lengthening per molecule and persistence length was not determined in these studies. Dietercalinium, a bis-intercalator (bivalent cationic above pH 7.5, tetravalent cationic below pH 7.5), increased the contour length and doubled the persistence length of DNA at saturating concentrations [33]. In a recent AFM study of monovalent cationic mono-intercalators ethidium bromide and doxorubicin, Cassina et al. [43] showed an increase in the contour length, but a decrease in the persistence length at higher doses of these molecules. In the same study, netropsin, a dicationic minor groove binder (not an intercalator), did not cause a significant change in contour length, but also decreased the persistence length by a factor of ~3. The decrease in the persistence length may be attributed to the positive charges on ethidium bromide and doxorubicin [44], and netropsin (dicationic) [45], which reduce the intramolecular electrostatic repulsion within the DNA molecule. Using laser tweezers, Baumann et al. [46] showed reduced stiffness in DNA due to interaction with monovalent and multivalent cations. Shiu et al. [47] suggest that in high charge intercalators (2+ or higher), the electrostatic interactions play a larger role in complex stability and may cause some unstacking, whereas in low charge intercalators stacking interactions appear to dominate the stability of the intercalator. Thus, in conclusion, it

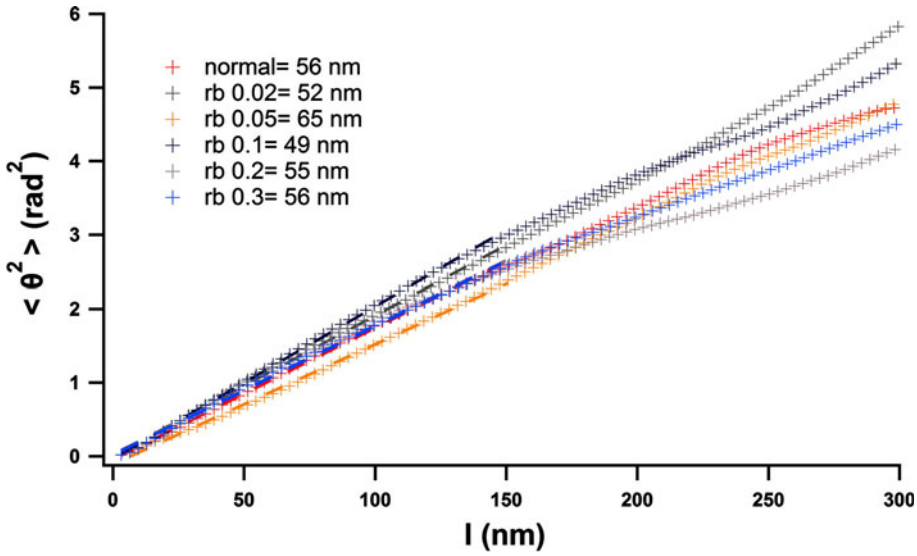

Fig. 6 Plot of $< \theta^2 >$ between two segments versus their separation distance, *l*. The analysis was performed for untreated DNA and DNA treated with different doses of PT-ACRAMTU ($r_b = 0$–0.3). The slope of this graph (*fitted, dashed lines*) is the inverse of the persistence length. The slope was evaluated for 3 nm $< l <$ 150 nm to avoid end effects

appears that each intercalator needs to be analyzed individually in terms of their effect on the DNA structure, stability and DNA persistence length. Some intercalators increase the persistence length (dietercalinium), while others reduce the persistence length (ethidium bromide, doxorubicin). Clearly, the detailed binding mode and associated charges play a critical role in the effect of an intercalator on DNA conformation.

The results of our AFM-based study are consistent with the finding that the anti-tumor drug PT-ACRAMTU interacts with DNA through a dual mechanism involving intercalation and covalent mono-adduct formation [15, 23]. We have studied the conformational transformation in DNA for varying concentrations of PT-ACRAMTU by measuring the contour length, *L*, persistence length, *P*, and aggregation. *L* was measured directly from the coordinate files of the AFM images, *P* was determined using the WLC model. DNA molecules lose one degree of freedom during their transformation from solution to a 2-D mica surface. Rivetti et al. [22, 48] showed that under favorable ionic conditions (2 mM Mg^{2+} buffer) DNA equilibrates on a 2-D mica surface resulting in a worm-like chain (WLC). Since the AFM images of DNA molecules represent an ensemble of low energy conformations, important structural information of these molecules can be extracted from their AFM images by studying them as WLC.

Increasing concentrations of PT-ACRAMTU resulted in the formation of some intrastrand DNA loops (Fig. 2g, h), and some intermolecular DNA aggregates. The likely reason for the formation of the DNA loops is the 2+ charge on the PT-ACRAMTU; the interaction of one molecule of PT-ACRAMTU neutralizes or reduces the negative charge on each base pair, resulting in the formation of loops within the DNA molecule. This hypothesis is in agreement with the observation that intermolecular DNA aggregates were observed for higher concentration of PT-ACRAMTU. The 2+ charge on PT-ACRAMTU may behave like a divalent ion which can link two DNA strands; several of these interactions could cause the formation of DNA aggregates as observed in Fig. 2e, f. Aggregation and condensation of DNA by multivalent cations, including cationic intercalators [49], is a known and well-described phenomenon [50].

One of the signature effects observed in DNA intercalators is that they increase the contour length of the DNA due to the stacking of the intercalating agent between two DNA base pairs [33, 51, 52]. The intercalation of PT-ACRAMTU in DNA increases the contour length by up to 0.6 nm/drug molecule before reaching a saturation phase at 15 % PT-ACRAMTU-to-DNA base pair ratio (Figs. 2, 4). Such a large increase in contour length was unexpected. The rise (distance between base pairs) is 0.34 nm per base pair in double-stranded DNA, and 0.7 nm per base in single-stranded DNA. Thus, by extending one stacked, double-stranded base pair to single-stranded DNA would only yield a difference of 0.36 nm (0.7–0.34 nm). The observation that adding a PT-ACRAMTU molecule increases the contour length by 0.6 nm implies that inserting a single PT-ACRAMTU molecule between stacked bases must also affect the adjacent bases and increase their spacing. Thus, PT-ACRAMTU may alter the spacing and geometry of three or more stacked base pairs. PT-ACRAMTU preferentially binds by intercalating between the 5′-CG-3′ and 5′-TA-3′ motif together with formation of a mono-adduct with the N7, N3, N1 of the guanine and adenine [15]. 80 and 11 % of adducts formed by PT-ACRAMTU is with the N7 atom of guanine and adenine in the major grove, respectively [15]. PT-ACRAMTU can also form a mono-adduct (7 %) with the N3 atom in the minor groove; a rare 2 % of adducts are formed due to its interaction with the N1 atom of adenine in the

major groove [15]. The saturation in the lengthening of DNA at 15 % PT-ACRAMTU to base pair ratio (1 drug per 6.7 base pairs) indicates the occupation of all binding sites in DNA by PT-ACRAMTU. An increase in the length of the DNA with an increase in PT-ACRAMTU dose is due to the intercalation of the planar acridine moiety between the DNA base pair. Below saturation, the obtained 0.6 nm/bp increase in DNA length is more than the stretchable width of a base pair, 0.34 nm/bp, and the typically observed increase of other DNA mono-intercalators. Previous NMR studies show that PT-ACRAMTU increased the contour length of DNA by about 0.34 nm/bp [13]. However, these studies were performed on a short DNA fragment (8 base pairs) containing a central 5′-CG-3′ adduct. A recent study of the PT-ACRAMTU interaction with calf thymus DNA [14] showed that the acridine moiety significantly deviates from co-planarity within the DNA intercalating pocket. Our results also suggest that the intercalation of the acridine moiety within the DNA base pair might not be planar and, in fact, may also increase the spacing between adjacent bases.

The flexibility of the DNA can be quantified by calculating P, and we determined P by extracting the persistence length of DNA from a plot of $< \theta^2 >$ versus l. Our results, summarized in Table 1, indicate that the DNA does not undergo a significant change in its flexibility due to its interaction with PT-ACRAMTU. This finding is also somewhat unexpected, since other intercalators change DNA stiffness, as discussed above. We suggest that two types of mechanical changes associated with the PT-ACRAMTU/DNA interaction may counterbalance each other. An increase in the rigidity of the DNA due to PT-ACRAMTU mono-adduct formation and intercalation could be offset by the reduced electrostatic repulsion between phosphate groups due to the 2+ charge of PT-ACRAMTU.

It should be noted that DNA molecules that were looped or aggregated were excluded from this analysis, since it was not possible to determine their contour length unequivocally. If those molecules could have been included, the persistence length for the aggregated molecules would have been shorter. We do not believe that looping and aggregation occurs because the DNA becomes softer. Instead, we believe that looping and aggregation occurs via unbound, dicationic PT-ACRAMTU molecules that form a bridge between different, negatively charged DNA molecules.

In summary, PT-ACRAMTU is distinct from other platinum cancer drugs, such as cisplatin, because it forms a mono-adduct, it intercalates, and it does not significantly bend the DNA, whereas cisplatin forms cross-links that bend the DNA by approximately 34°. PT-ACRAMTU is also distinct from other intercalators, which are typically reversible binders, because it forms an irreversible covalent mono-adduct. This binding mode does not change the persistence length of DNA, whereas many other intercalators do not form covalent bonds, but they change (increase or decrease) the persistence length of DNA significantly. The unique DNA damage mechanism of PT-ACRAMTU and its second-generation derivatives appears to be a key event in producing efficient cell death in chemoresistant cancers.

Acknowledgments We thank Lu Rao for technical support with DNA-drug incubations. This work was supported by the National Science Foundation [CMMI-0646627, to M.G.], the North Carolina Biotechnology Center [2011-MRG-1115, to M.G.], and the National Institutes of Health [CA101880, to U.B.].

References

1. Eastman, A. (1990). Activation of programmed cell death by anticancer agents—cisplatin as a model system. *Cancer Cells-A Monthly Review, 2*, 275–280.
2. Chaney, S. G., Campbell, S. L., Temple, B., Bassett, E., Wu, Y. B., & Faldu, M. (2004). Protein interactions with platinum-DNA adducts: From structure to function. *Journal of Inorganic Biochemistry, 98*, 1551–1559.
3. Kartalou, M., & Essigmann, J. M. (2001). Mechanisms of resistance to cisplatin. *Mutation Research-Fundamental and Molecular Mechanisms of Mutagenesis, 478*, 23–43.
4. Einhorn, L. H. (2002). Curing metastatic testicular cancer. *Proceedings of the National Academy of Sciences of the United States of America, 99*, 4592–4595.
5. Takahara, P. M., Frederick, C. A., & Lippard, S. J. (1996). Crystal structure of the anticancer drug cisplatin bound to duplex DNA. *Journal of the American Chemical Society, 118*, 12309–12321.
6. Takahara, P. M., Rosenzweig, A. C., Frederick, C. A., & Lippard, S. J. (1995). Crystal-structure of double-stranded DNA containing the major adduct of the anticancer drug cisplatin. *Nature, 377*, 649–652.
7. Rosell, R., Lord, R. V. N., Taron, M., & Reguart, N. (2002). DNA repair and cisplatin resistance in non-small-cell lung cancer. *Lung Cancer, 38*, 217–227.
8. Martins, E. T., Baruah, H., Kramarczyk, J., Saluta, G., Day, C. S., Kucera, G. L., et al. (2001). Design, synthesis, and biological activity of a novel non-cisplatin-type platinum-acridine pharmacophore. *Journal of Medicinal Chemistry, 44*, 4492–4496.
9. Hess, S. M., Mounce, A. M., Sequeira, R. C., Augustus, T. M., Ackley, M. C., & Bierbach, U. (2005). Platinum-acridinylthiourea conjugates show cell line-specific cytotoxic enhancement in H460 lung carcinoma cells compared to cisplatin. *Cancer Chemotherapy and Pharmacology, 56*, 337–343.
10. Ma, Z., Choudhury, J. R., Wright, M. W., Day, C. S., Saluta, G., Kucera, G. L., et al. (2008). A non-cross-linking platinum-acridine agent with potent activity in non-small-cell lung cancer. *Journal of Medicinal Chemistry, 51*, 7574–7580.
11. Baruah, H., Rector, C. L., Monnier, S. M., & Bierbach, U. (2002). Mechanism of action of non-cisplatin type DNA-targeted platinum anticancer agents: DNA interactions of novel acridinylthioureas and their platinum conjugates (vol 64, pg 191, 2002). *Biochemical Pharmacology, 64*, 751.
12. Budiman, M. E., Bierbach, U., & Alexander, R. W. (2005). Minor groove adducts formed by a platinum-acridine conjugate inhibit association of TATA-binding protein with its cognate sequence. *Biochemistry, 44*, 11262–11268.

13. Baruah, H., Wright, M. W., & Bierbach, U. (2005). Solution structural study of a DNA duplex containing the guanine-N7 adduct formed by a cytotoxic platinum-acridine hybrid agent. *Biochemistry, 44*, 6059–6070.
14. Kostrhunova, H., Malina, J., Pickard, A. J., Stepankova, J., Vojtiskova, M., Kasparkova, J., et al. (2011). Replacement of a thiourea with an amidine group in a monofunctional platinum-acridine antitumor agent. Effect on DNA interactions, DNA adduct recognition and repair. *Molecular Pharmaceutics, 8*, 1941–1954.
15. Barry, C. G., Day, C. S., & Bierbach, U. (2005). Duplex-promoted platination of adenine-N3 in the minor groove of DNA: Challenging a longstanding bioinorganic paradigm. *Journal of the American Chemical Society, 127*, 1160–1169.
16. Wang, H., Yang, Y., Schofield, M. J., Du, C. W., Fridman, Y., Lee, S. D., et al. (2003). DNA bending and unbending by MutS govern mismatch recognition and specificity. *Proceedings of the National Academy of Sciences of the United States of America, 100*, 14822–14827.
17. Perez-Lago, L., Salas, M., & Camacho, A. (2005). A precise DNA bend angle is essential for the function of the phage phi 29 transcriptional regulator. *Nucleic Acids Research, 33*, 126–134.
18. Wuite, G. J. L., Smith, S. B., Young, M., Keller, D., & Bustamante, C. (2000). Single-molecule studies of the effect of template tension on T7 DNA polymerase activity. *Nature, 404*, 103–106.
19. Bustamante, C., Bryant, Z., & Smith, S. B. (2003). Ten years of tension: Single-molecule DNA mechanics. *Nature, 421*, 423–427.
20. Erie, D. A., Yang, G. L., Schultz, H. C., & Bustamante, C. (1994). DNA bending by Cro protein in specific and nonspecific complexes—implications for protein site recognition and specificity. *Science, 266*, 1562–1566.
21. Hou, X.-M., Zhang, X.-H., Wei, K.-J., Ji, C., Dou, S.-X., Wang, W.-C., et al. (2009). Cisplatin induces loop structures and condensation of single DNA molecules. *Nucleic Acids Research, 37*, 1400–1410.
22. Rivetti, C., Guthold, M., & Bustamante, C. (1996). Scanning force microscopy of DNA deposited onto mica: Equilibration versus kinetic trapping studied by statistical polymer chain analysis. *Journal of Molecular Biology, 264*, 919–932.
23. Barry, C. G., Baruah, H., & Bierbach, U. (2003). Unprecedented monofunctional metalation of adenine nucleobase in guanine- and thymine-containing dinucleotide sequences by a cytotoxic platinum-acridine hybrid agent. *Journal of the American Chemical Society, 125*, 9629–9637.
24. Rivetti, C., Walker, C., & Bustamante, C. (1998). Polymer chain statistics and conformational analysis of DNA molecules with bends or sections of different flexibility. *Journal of Molecular Biology, 280*, 41–59.
25. Baruah, H., & Bierbach, U. (2004). Biophysical characterization and molecular modeling of the coordinative-intercalative DNA monoadduct of a platinum-acridinylthiourea agent in a site-specifically modified dodecamer. *Journal of Biological Inorganic Chemistry, 9*, 335–344.
26. Choudhury, J. R., Rao, L., & Bierbach, U. (2011). Rates of intercalator-driven platination of DNA determined by a restriction enzyme cleavage inhibition assay. *Journal of Biological Inorganic Chemistry, 16*, 373–380.
27. Landau, L. D., Lifshitz, E. M. (1980). *Statistical physics* Part 1. 3rd edn.
28. Kratky, O., Porod, G. (1949). Röntgenuntersuchungaufgelöster Fadenmoleküle. Recueil 68:1106–1122.
29. Schellman, J. A. (1974). Flexibility of DNA. *Biopolymers, 13*, 217–226.
30. Frontali, C. (1988). Excluded-volume effect on the bidimensional conformation of DNA molecules adsorbed to protein films. *Biopolymers, 27*, 1329–1331.
31. Flory, P. J. (1969). *Statistical mechanics of chain molecules*. New York: Interscience Publishers.
32. Bettini, A., Pozzan, M. R., Valdevit, E., & Frontali, C. (1980). Microscopic persistence length of DNA: Its relation to average molecular dimensions. *Biopolymers, 19*, 1689–1694.
33. Berge, T., Jenkins, N. S., Hopkirk, R. B., Waring, M. J., Edwardson, J. M., & Henderson, R. M. (2002). Structural perturbations in DNA caused by bis-intercalation of ditercalinium visualised by atomic force microscopy. *Nucleic Acids Research, 30*, 2980–2986.
34. Marshall, L. E., Graham, D. R., Reich, K. A., & Sigman, D. S. (1981). Cleavage of deoxyribonucleic acid by the 1, 10 phenanthroline-cuprous complex—hydrogen peroxide requirement and primary and secondary structure specificity. *Biochemistry, 20*, 244–250.
35. Guirouilh-Barbat, J., Zhang, Y.-W., & Pommier, Y. (2009). Induction of glutathione-dependent DNA double-strand breaks by the novel anticancer drug brostallicin. *Molecular Cancer Therapeutics, 8*, 1985–1994.
36. Cai, H–. H., Yang, P.-H., Chen, J., Liang, Z.-H., Chen, Q., & Cai, J. (2009). Visual characterization and quantitative measurement of artemisinin-induced DNA breakage. *Electrochimica Acta, 54*, 3651–3656.
37. Bustamante, C., Marko, J. F., Siggia, E. D., & Smith, S. (1994). Entropic elasticity of lambda-phage DNA. *Science, 265*, 1599–1600.
38. Smyre, C. L., Saluta, G., Kute, T. E., Kucera, G. L., & Bierbach, U. (2011). Inhibition of DNA synthesis by a platinum–acridine hybrid agent leads to potent cell kill in nonsmall cell lung cancer. *Acs Medicinal Chemistry Letters, 2*, 870–874.
39. Coury, J. E., McFailIsom, L., Williams, L. D., & Bottomley, L. A. (1996). A novel assay for drug-DNA binding mode, affinity, and exclusion number: Scanning force microscopy. *Proceedings of the National Academy of Sciences of the United States of America, 93*, 12283–12286.
40. Mihailovic, A., Vladescu, L., McCauley, M., Ly, E., Williams, M. C., Spain, E. M., et al. (2006). Exploring the interaction of ruthenium(II) polypyridyl complexes with DNA using single-molecule techniques. *Langmuir, 22*, 4699–4709.
41. Tseng, Y. D., Ge, H. F., Wang, X. Z., Edwardson, J. M., Waring, M. J., Fitzgerald, W. J., et al. (2005). Atomic force microscopy study of the structural effects induced by echinomycin binding to DNA. *Journal of Molecular Biology, 345*, 745–758.
42. Bordelon, J. A., Feierabend, K. J., Siddiqui, S. A., Wright, L. L., & Petty, J. T. (2002). Viscometry and atomic force microscopy studies of the interactions of a dimeric cyanine dye with DNA. *Journal of Physical Chemistry B, 106*, 4838–4843.
43. Cassina, V., Seruggia, D., Beretta, G. L., Salerno, D., Brogioli, D., Manzini, S., et al. (2011). Atomic force microscopy study of DNA conformation in the presence of drugs. *European Biophysics Journal with Biophysics Letters, 40*, 59–68.
44. Langner, K. M., Kedzierski, P., Sokalski, W. A., & Leszczynski, J. (2006). Physical nature of ethidium and proflavine interactions with nucleic acid bases in the intercalation plane. *Journal of Physical Chemistry B, 110*, 9720–9727.
45. Dolenc, J., Oostenbrink, C., Koller, J., & van Gunsteren, W. F. (2005). Molecular dynamics simulations and free energy calculations of netropsin and distamycin binding to an AAAAA DNA binding site. *Nucleic Acids Research, 33*, 725–733.
46. Baumann, C. G., Smith, S. B., Bloomfield, V. A., & Bustamante, C. (1997). Ionic effects on the elasticity of single DNA molecules. *Proceedings of the National Academy of Sciences of the United States of America, 94*, 6185–6190.
47. Shui, X. Q., Peek, M. E., Lipscomb, L. A., Gao, Q., Ogata, C., Roques, B. P., et al. (2000). Effects of cationic charge on three-dimensional structures of intercalative complexes: Structure of a

bis-intercalated DNA complex solved by MAD phasing. *Current Medicinal Chemistry, 7*, 59–71.
48. Sushko, M. L., Shluger, A. L., & Rivetti, C. (2006). Simple model for DNA adsorption onto a mica surface in 1:1 and 2:1 electrolyte solutions. *Langmuir, 22*, 7678–7688.
49. Bhat, S. S., Kumbhar, A. S., Kumbhar, A. A., & Khan, A. (2012). Efficient DNA condensation induced by Ruthenium(II) complexes of a bipyridine-functionalized molecular clip ligand. *Chemistry-A European Journal, 18*, 16383–16392.
50. Bloomfield, V. A. (1996). DNA condensation. *Current Opinion in Structural Biology, 6*, 334–341.
51. Utsuno, K., Tsuboi, M., Katsumata, S., & Iwamoto, T. (2001). Viewing of complex molecules of ethidium bromide and plasmid DNA in solution by atomic force microscopy. *Chemical and Pharmaceutical Bulletin, 49*, 413–417.
52. Berge, T., Haken, E. L., Waring, M. J., & Henderson, R. M. (2003). The binding mode of the DNA bisintercalator luzopeptin investigated using atomic force microscopy. *Journal of Structural Biology, 142*, 241–246.